Influence of the Support on the Structural Characteristics of Carbon Nanofibers Produced from the Metal-Catalyzed Decomposition of Ethylene

Paul E. Anderson and Nelly M. Rodríguez*

Department of Chemistry, Northeastern University, Boston, Massachusetts 02115

Received September 10, 1999. Revised Manuscript Received December 20, 1999

The notion of using support materials to achieve high dispersions of metal particles has been extended to the synthesis of carbon nanofibers from the catalyzed decomposition of ethylene. By using this approach it has been possible to generate nanofibers whose widths are dictated by the dimensions of the supported metal particles. In addition, the support may alter the state of the bulk and/or the surface of the catalyst particle through metal−support interactions, and the impact of this effect is manifested by modifications in the structural characteristics of the nanofiber deposits. In an attempt to gain a clearer insight into the influence of metal−support interaction on the growth characteristics of GNF, three metals, Fe, Ni, and Co that are known to be active catalysts for this process were impregnated onto silica, graphite, and well-characterized graphite nanofiber supports. Characterization of the solid carbon products was performed by a variety of approaches including high-resolution transmission electron microscopy (HRTEM), gas-phase analysis, and thermal-programmed oxidation (TPO). The goal of this study was to correlate each nanofiber product with the behavior of the specific metal/support precursor system. The advantages of using selected support materials to control the morphologies and sizes of nanofibers is presented.

Introduction

The formation of carbon nanofibers during the interaction of carbon-containing gases with hot metal surfaces has been known for decades and considerable effort has been expended in attempts to prevent the collection of this material as it can have deleterious effects with regard to the efficient operation of many processes.[1−5] In recent years, however, it has been recognized that by judicious selection of a metal catalyst particle, coupled with a strict control of the composition of the reactant gas and the temperature, it is possible to tailor the structure of the carbonaceous material and generate an assortment of structures.[6,7] Of the many conformations that it is possible to produce by altering the catalyst and the reaction parameters, two types have received a great deal of attention; the tubular type or "nanotube", because it is anticipated that they may have a variety of applications,[8−10] and those with only edges exposed because they can store vast amounts of hydrogen.[11] It is interesting to note that many of these materials consist entirely of graphite and can be produced at 600−700 °C, conditions well below the temperatures necessary for graphitization (∼2700 °C).

Baker and co-workers[12] developed a mechanism for the metal-catalyzed growth of carbon nanofibers based on dynamic studies performed by controlled atmosphere electron microscopy (CAEM). The principal steps of this mechanism involved the decomposition of a hydrocarbon on specific surfaces of the metal to generate carbon species that subsequently dissolved and diffused through the bulk and were eventually deposited as a fibrous structure on a different set of crystallographic faces of the particle. It has been shown that the crystallographic orientation of the depositing faces of the particle plays a crucial role in determining the degree of crystallinity of the carbon structure. For example, the interstitial spaces between atoms in the Ni (111) face indeed coincide very closely with the carbon−carbon spacing of graphite, and hence a Ni (111) face preferentially precipitates graphitized carbon.[13]

While many workers have investigated the formation of nanofibers from catalyzed decomposition of carbon-containing gases over various metals and alloys,[14−19] there has been no systematic study of the influence of the support medium on the structural characteristics

* To whom all inquiries should be addressed.

(1) Everett, M. R.; Kinsey, D. V.; Romberg, E. In *Chemistry and Physics of Carbon*; Walker, P. L., Jr., Ed.; Marcel Dekker: New York, 1968; Vol. 3, p 289.
(2) Baker, R. T. K.; Harris, P. S. P. A. In *Chemistry and Physics of Carbon*; Walker, P. L., Jr., Ed.; Thrower, P. A.; Marcel Dekker: New York, 1978; Vol. 14, p 83.
(3) Rostrup-Nielsen, J. R. *Steam Reforming Catalysts*; Danish Technical Press: Copenhagen, 1975.
(4) Trimm, D. L. *Catal. Rev. Sci. Eng.* **1977**, *16*, 155.
(5) Albright, L. F.; Baker, R. T. K. *Coke Formation on Metal Surfaces*; ACS Symposium Series 202; American Chemical Society: Washington, DC, 1982.
(6) Rodriguez, N. M. *J. Mater. Res.* **1993**, *8*, 3233.
(7) Rodriguez, N. M.; Chambers, A.; Baker, R. T. K. *Langmuir* **1995**, *11*, 3862.
(8) Iijima, S. *Nature* **1991** *354*, 56.
(9) Bethune, D. S.; Kiang, C. H.; deVries, M. S.; Gorman, G.; Savoy, R.; Vazquez, J.; Beyers, R. *Nature* **1993**, *363*, 605.
(10) Dai, H., Rinzler, A. G.; Nikolaev, P., Thess, A.; Colbert, D. T.; Smalley, R. E. *Chem. Phys. Lett.* **1996** *260*, 471.
(11) Chambers, A.; Park, C.; Baker, R. T. K.; Rodriguez, N. M. *J. Phys. Chem.* **1998**, *102*, 4253.
(12) Baker, R. T. K.; Barber, M. A.; Harris, P. S.; Feates, F. S.; Waite, R. J. *J. Catal.* **1972**, *26*, 51.
(13) Yang, R. T.; Chen, J. P. *J. Catal.* **1989**, *115*, 52.

10.1021/cm990582n CCC: $19.00
Published on Web 02/12/2000

of the carbonaceous solid when the metal particles are dispersed on a carrier. There are reports in the literature where carbon nanofibers have been grown from the interaction of various hydrocarbon/hydrogen mixtures with iron salts dispersed on graphite foils.[20−23] When the metal catalyst is supported on a suitable material, the orientation of the particle surface is quite different to that encountered with a pure powdered metal sample and as a consequence, the reactivity pattern toward certain gases is dramatically perturbed. The nature and strength of the interaction between the two components may (a) induce electronic perturbations throughout the metal,[24,25] (b) generate significant differences in the metal morphology and the arrangement of the surface atoms,[26,27] (c) exert an influence on the growth characteristics of the supported metal particles,[28,29] and (d) in some cases, modify the chemistry of the system as a result of migration of support species onto the surface of the metal.[30]

The interactions of a metal particle with graphite are quite different to those observed with either silica or alumina, which is expected, since with the former material we are dealing with an electrical conductor, whereas the refractory oxides are insulators. Furthermore, graphite possesses a well defined structure with a high degree of crystallinity, whereas the oxides have only short range order and are mostly amorphous. A review of the studies on catalytic gasification of graphite performed with the CAEM technique provides direct insights into the qualitative aspects surrounding the interactions of a number of metals in the presence of various gases.[31] One of the most significant results of these investigations was the observation that for catalyzed gasification to occur, the metal particles must be located on the graphite edge sites, indicating that these are the most active regions. It was also demonstrated that the onset and mode of catalytic attack were directly related to the ability of the metal particles to undergo a wetting action with the graphite edges, a phenomenon that was dictated by the strength of the interaction between the two surfaces.[32,33]

Table 1. Characteristics of the Support Media

support	surface area N_2 BET m^2/g	geometric properties	electronic properties
SiO_2	255	amorphous	insulator
SP1 graphite	6	∼5% edge sites	conductor in basal plane
platelet GNF	234	∼99% edge sites	conductor (basal plane) and semiconductor (along edges)

If the above criteria are extended to the area of nanofiber synthesis, it becomes clear that differences in the nature of the interaction between the metal catalyst particles and the support are going to be reflected in variations of the growth characteristics in the carbon structures. In the extreme case, when a strong interaction exists between the metal catalyst and the support, subsequent growth of nanofibers will occur via an extrusion mode, where the particle remains firmly attached to the carrier throughout the reaction sequence.[34] This study provides a direct comparison of the structural characteristics of carbon nanofibers produced from different supported metal systems and lends insight into the impact of the strength of metal/support interaction on the growth process. As the catalytic formation of GNFs and nanotubes becomes an increasingly attractive route for production of these types of materials, it is essential that one is able to control both the size and morphological features of the metal catalyst particle. The logical method to achieve this goal is through a fundamental understanding of the nature of the metal/support interaction.

Experimental Section

Catalyst Preparation. Three different types of support materials were selected: Cab-o-Sil amorphous fumed silica, SP1 Graphite obtained from Alfa Aesar (where the percent exposed basal plane to edge area was over 95%) and platelet graphite nanofibers (where the percent exposed edge to basal plane area was over 99%). The "platelet" graphite nanofibers were prepared according to the procedure outlined in a previous paper.[35] Prior to use, the graphite nanofibers (GNF) were treated in 1 M hydrochloric acid for a week to remove the iron catalyst. The characteristics of the three support materials are given in Table 1. Iron, cobalt, and nickel were separately introduced onto each of the graphitic supports via incipient wetness impregnation in ethanol using the respective metal nitrates as precursor salts to produce a 5 wt % metal loading. The impregnated materials were all dried overnight in air at 110 °C, followed by calcination in air at 350 °C for 4 h and finally reduced in 10% H_2/He at 350 °C for 24 h. The corresponding silica supported catalyst systems were prepared according to a similar protocol; however, in these cases it was necessary to treat the samples for 36 h in a 10% H_2/He stream at 350 °C to ensure complete reduction of the particles to the metallic state. All catalysts were cooled to room temperature, and passivated in 2% air/He for 2 h prior to removal from the reactor. These treatments and the subsequent carbon deposition reactions were performed in a horizontal flow reactor system. All gas flow rates were regulated with MKS mass flow controllers.

Carbon Nanofiber Growth Protocol. Approximately 150 mg of a given catalyst sample was uniformly dispersed along

(14) Sacco, A. In *Carbon Fibres, Filaments and Composites*; Figueiredo, J. L., et al., Eds.; Kluwer Academic: Amsterdam, 1990; p 459.
(15) Nishiyama, Y.; Tamai, Y. *J. Catal.* **1974**, *33*, 98.
(16) Audier, M.; Guinot, J.; Coulon, M.; Bonnetain, L. *Carbon* **1981**, *19*, 99.
(17) De Bokx, P. K.; Kock, A. J. H. M.; Boellaard, E.; Klop, W.; Geus, J. W. *J. Catal.* **1985**, *96*, 454.
(18) Kim, M. S.; Rodriguez, N. M.; Baker, R. T. K. *J. Catal.* **1991**, *131*, 60.
(19) Krishnankutty, N.; Park, C.; Rodriguez, N. M.; Baker, R. T. K. *Catal. Today* **1997**, *37*, 295.
(20) Benissad, F.; Gadelle, P.; Coulon, M.; Bonnetain, L. *Carbon* **1988**, *26*, 61.
(21) Benissad, F.; Gadelle, P.; Coulon, M.; Bonnetain, L. *Carbon* **1989**, *27*, 585.
(22) Benissad, F.; Gadelle, P. *Carbon* **1993**, *31*, 21.
(23) Jose-Yacaman, M.; Miki-Yoshida, M.; Rendon, L.; Santiesteban, J. G. *Appl. Phys. Lett.* **1993**, *62*, 657.
(24) Rodriguez, J. A.; Goodman, D. W. *J. Phys. Chem.* **1991**, *95*, 4196.
(25) Kuhn, W. K.; Campbell, R. A.; Goodman, D. W. In *The Chemical Physics of Solid Surfaces*; Elsevier: Amsterdam, 1993; p 157.
(26) Pilliar, R. M.; Nutting, J. *Philos. Mag.* **1967**, *6*, 181.
(27) Baker, R. T. K.; Prestridge, E. B.; Garten, R. L. *J. Catal.* **1979**, *56*, 390.
(28) Chen, J. J.; Ruckenstein, E. *J. Catal.* **1981**, *69*, 254.
(29) Arai, M.; Ishikawa, T.; Nakayama, T.; Nishiyama, Y. *J. Colloid Interface Sci.* **1984**, *97*, 254.
(30) Dumesic, J. A.; Stevenson, S. A.; Sherwood, R. D.; Baker, R. T. K. *J. Catal.* **1986**, *99*, 79.
(31) Baker, R. T. K. *J. Adhes.* **1995**, *52*, 13.
(32) Baker, R. T. K.; Sherwood, R. D. *J. Catal.* **1981**, *70*, 198.
(33) Baker, R. T. K.; Chludzinski, J. J. *Carbon* **1981**, *19*, 75.
(34) Baker, R. T. K.; Chludzinski, J. J. *J. Phys. Chem.* **1986**, *90*, 4734.
(35) Rodriguez, N. M.; Kim, M. S.; Baker, R. T. K. *J. Catal.* **1993**, *144*, 93.

Table 2. Percent by Weight Carbon Deposition after 90-min Reaction in C_2H_4/H_2 (4:1) at 600 °C

	support		
metal	SP1 graphite	silica	platelet GNF
5% nickel	84.0	78.0	78.0
5% cobalt	13.0	4.0	34.0
5% iron	20.0	19.0	69.0

the base of a ceramic boat and placed in the center of the reactor. Initially the catalyst was reduced for 2 h in a 20% H_2/He stream at 600 °C to ensure the passivated particles were converted to the metallic state. After the system was flushed with 100 mL/min He at 600 °C for 1 h, a 80/20 mL/min C_2H_4/H_2 reactant mixture was introduced into the system. The composition of the reactant gas was analyzed at the start and at regular intervals during the reaction with a Varian 3400 gas chromatography unit using a 30 m megabore column (GS-Q). Carbon and hydrogen atom balances in conjunction with the relative concentrations of the respective components were employed to calculate the solid carbon yields as a function of time. The reaction was allowed to proceed for 1.5 h and at the completion of the experiment the system was cooled to room temperature in 100 mL/min He; the solid product was weighed and stored for further characterization. In all cases the computed and measured weights of the solid carbon product were within ±5%.

The gases used in this work, ethylene (99.95%), hydrogen (99.99%), and helium (99.999%) were obtained from Med Tech Industries and used without further purification. Reagent-grade iron nitrate [$Fe(NO_3)_3 \cdot 9H_2O$], nickel nitrate [$Ni(NO_3)_2 \cdot 6H_2O$], and cobalt nitrate [$Co(NO_3)_2 \cdot 6H_2O$] were purchased from Fisher Scientific for the catalyst preparation.

Characterization Studies. The structural details of the solid carbon deposits were obtained from transmission electron microscopy (TEM) studies. The determinations of catalyst particle size distributions (PSD) and associated nanofiber size distributions (FSD) were performed on a JEOL 100 CX instrument and these data were collected from the widest points on the particle/nanostructure interface regions. High-resolution TEM (HRTEM) examinations were carried out on a JEOL 2010 FX instrument, capable of 0.18 nm lattice resolution. Representative specimens of the deposits produced from each experiment were prepared by ultrasonic dispersion of the carbonaceous material in isobutyl alcohol and then application of a drop of the supernate onto a holey carbon film.

An estimate of the overall degree of the graphitic nature of the carbon deposit produced on the silica supported metal systems was obtained from a comparison of the oxidation profile (weight loss as a function of reaction temperature) of the material in CO_2/Ar (1:1) with those found for two standards, single-crystal graphite and amorphous carbon, when treated under the same conditions. These experiments were conducted in a Cahn 2000 microbalance at a heating rate of 5 °C/min. To avoid ambiguities from the presence of metallic impurities all samples were treated in 1 M hydrochloric acid for a period of 1 week, a procedure that had previously been found to be very effective for the complete removal of the metal that could catalyze the oxidation of the carbon samples.[35]

Results

Solid Carbon Yield as a Function of Catalyst System. The percent yields of solid carbon as determined by the weight gain after reaction of the various catalyst systems in an ethylene/hydrogen (4:1) mixture for 90 min at 600 °C are given in Table 2. Inspection of these data shows that the yields of solid carbon were highest for the GNF-supported metals, followed by the corresponding SP1 graphite-supported systems, with the lowest performance being achieved when silica was used as the supporting medium. Of particular significance is the relatively high yield of nanofibers found for the iron/platelet GNF system, since in the unsupported condition iron does not readily dissociate ethylene and as a consequence, exhibits a poor performance for the growth of carbon nanofibers.

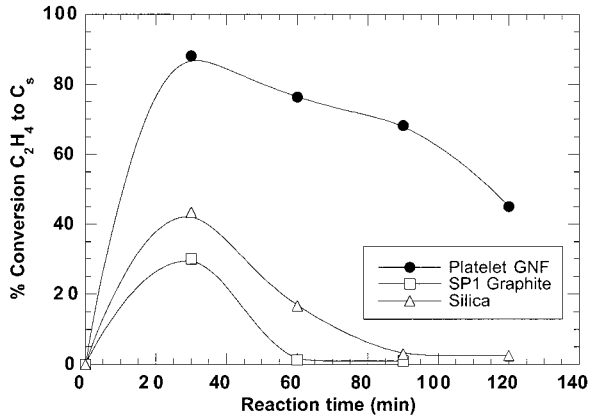

Figure 1. Comparison of the solid carbon yields from the decomposition of ethylene over the three supported iron catalysts at 600 °C as a function of time.

A comparison of the solid carbon yields from the decomposition of ethylene over the three supported iron catalysts as a function of time is presented in Figure 1. The maximum amount of nanofibers was not only higher when the metal was dispersed on the platelet GNF support, but the activity was maintained for a longer period in this system than when the same reaction was performed over either Fe/SP1 graphite or Fe/SiO_2 samples. The plots for the analogous supported nickel and cobalt catalysts were qualitatively similar to those for iron, but differed in the magnitude of the amounts of solid carbon that were formed.

Characterization of the Solid Carbon Deposit. *TEM Studies* Examination of the samples of solid carbon in the transmission electron microscope (TEM) indicated that in all cases the solid product consisted exclusively of carbon nanofibers. It was possible to establish a set of physical and structural characteristics of the nanofibers produced from a given catalyst system on the basis of a detailed survey of a number of fields of view of each specimen. A comparison of these observations showed that there were significant differences in the nature of the nanofibers generated from each supported metal system and moreover, such variations extended to the behavior of the same metal on different support media.

A typical width distribution of carbon nanofibers produced from the catalytic decomposition of ethylene/hydrogen (4:1) at 600 °C is shown in Figure 2 for the nickel/silica system. The corresponding data for all the other systems investigated in this work is given in Table 3, along with that from the respective unsupported metal systems. Examination of these data reveals that for the most part the width of nanofibers matched that of the catalyst particles with the exception of the iron/GNF system. Furthermore, nanofibers generated from the supported catalyst systems are, on average, smaller than those grown from the unsupported metal powders.

Iron particles that accumulated on the graphite edge sites tended to acquire a rectangular geometry, whereas particles in contact with the basal plane regions were smaller, but more globular in appearance. In the cobalt/graphite system a large fraction of relatively large rectangular shaped particles congregated on the edges

Table 3. Size Range of Particles and Associated Carbon Nanofibers Produced from the Various Metal Catalyst Systems

	average width (nm)						
	SP1 graphite		silica		platelet GNF		unsupported
metal	particles	fibers	particles	fibers	particles	fibers	fibers
Ni	3−47	3−50	5−46	4−49	2−40	5−50	35−450[18]
Co	4−40	4−49[a]	4−22	2−18	2−24	4−28	25−250[47]
Fe	3−50	4−35	5−35	3−20	3−35	20−150	—[b,35]

[a] A small fraction of larger fibers was also observed. [b] No fibers were produced from the reaction of C_2H_4 with unsupported Fe catalysts.

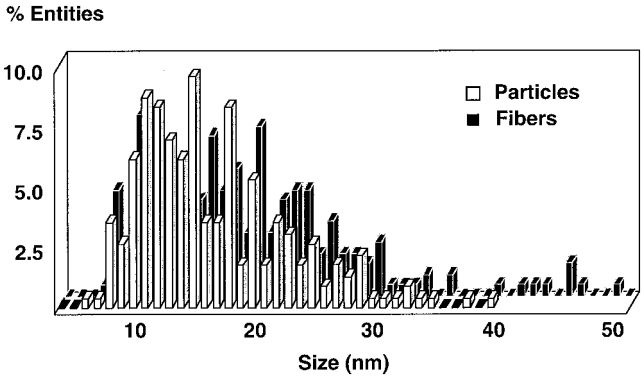

Figure 2. Width distribution of both particles and carbon nanofibers produced from the decomposition of C_2H_4/H_2 (4:1) over a nickel/silica catalyst at 600 °C.

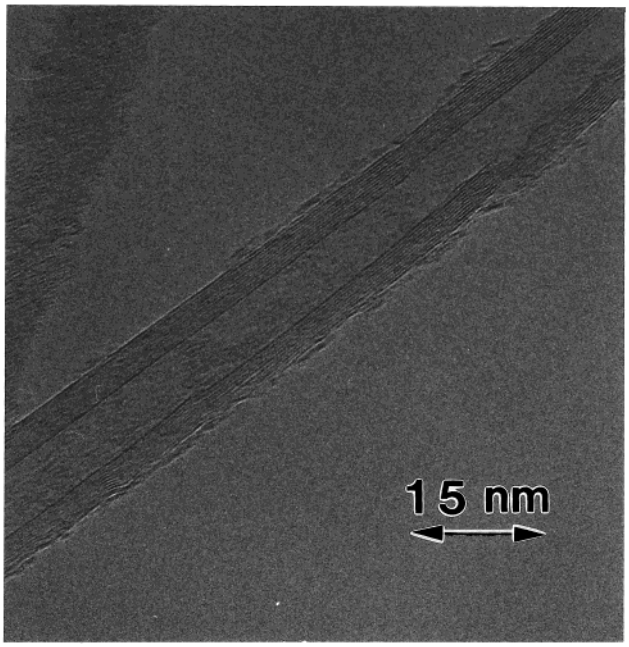

Figure 3. High-resolution electron micrograph showing the arrangement of the graphite sheets constituting the walls of the tubular nanofibers produced from the decomposition of C_2H_4/H_2 (4:1) over a iron/silica catalyst at 600 °C.

of the support and the basal planes were only sparsely covered with very small particles. With nickel, the particles adopted a faceted morphology and evenly dispersed over the entire basal plane surfaces. Although nickel is known to undergo a spreading action on the edges of graphite during treatment in hydrogen at 850 °C,[32] few particles were seen to have collected at these sites under the current reduction conditions.

Nanofiber surfaces were completely free of any extraneous material, indicating that uncatalyzed decomposition of ethylene, which would give rise to the deposition of amorphous carbon, was not taking place under the current experimental conditions. For the sake of clarity the specific structural features of the carbon nanofibers produced from the three metals are described separately in the following sections:

(a) Supported Iron Particles. Although SP1 and silica-supported iron particles were not very efficient catalysts for the growth of these types of carbon materials from ethylene, the nanofibers that were formed in these systems tended to be relatively uniform in size and acquired a tubular structure. It is significant that there was no evidence for the existence of metal particles either within the body or at the tips of the nanofibers produced from the iron/silica system. It is therefore possible that growth of these structures proceeded via an extrusion mode, where the iron particles remained attached to the support surface during the growth sequence. A further possibility is that the particles became dislodged upon cooling or during the ultrasonic dispersion step used in the specimen preparation procedure. In contrast, the iron/graphite and iron/platelet GNF systems generated nanofibers in which the metal particles were lifted away from the support indicative of a whiskerlike, rather than extrusion, mode of growth.

The GNF-supported iron catalyst was a particularly intriguing system in that the size distribution of the nanofibers was about an order of magnitude larger than that of the initial metal particles. It was evident, that during reaction with the ethylene/hydrogen mixture at 600 °C the iron particles underwent a change in morphological characteristics, manifested in the appearance of the nanofibers. A separate experiment was performed in which the GNF supported iron particles were treated in the presence of hydrogen at 600 °C. Subsequent examination by TEM showed the presence of very wide, flat particles, indications that a spreading action of the metal had occurred on the graphite edge regions. This catalyst system generated the highest yield of nanofibers among the supported iron systems.

High-resolution TEM investigations revealed additional details regarding the structural characteristics of the nanofibers. The graphite sheets constituting the walls of the tubular nanofibers produced from the iron/silica catalyst were parallel to the axis of growth. Furthermore, some of the nanofibers approached a very small size, having wall thicknesses of seven graphite layers, an aspect that can be seen in Figure 3. Sections of carbon nanofibers formed from the interaction of the hydrocarbon with graphite supported iron particles are shown in Figure 4. It is evident that once again the graphite platelets constituting the material are aligned in a direction parallel to the fiber axis. The subtle differences in the structure of the nanofibers achieved by supporting the iron particles on platelet GNF supports is evident in Figure 5. Here, the graphite sheets

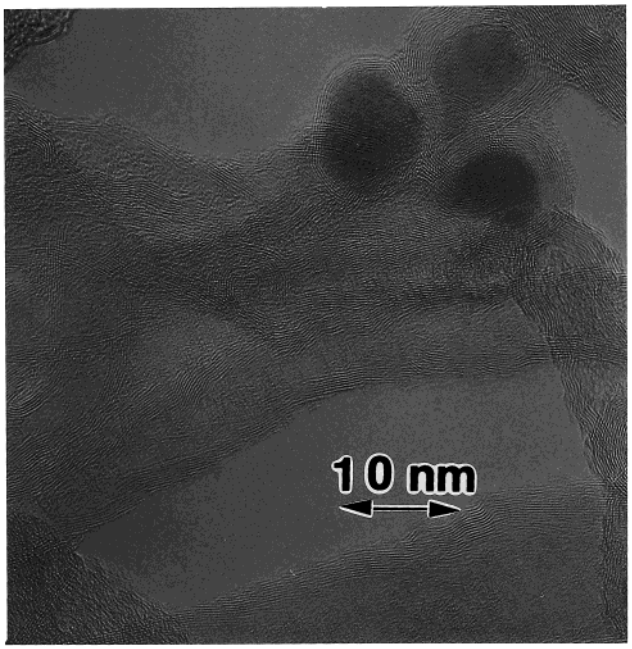

Figure 4. High-resolution electron micrograph of sections of carbon nanofibers formed from the interaction of C_2H_4/H_2 (4:1) with graphite-supported iron particles at 600 °C.

are aligned at some angle with respect to the fiber axis and give the appearance of a stack of cones.

Despite the differences in growth characteristics observed with the three supported iron catalysts in all these systems, the small diameter metal particles were capable of catalyzing the formation of extremely long nanofibers, typically up to 100 μm in length. The growth must occur very rapidly as the lifetime of an individual catalyst particle was relatively short.

(b) Supported Cobalt Particles. In the Co/SiO_2 system almost all of the particles were found to be encapsulated by graphite overlayers and this accounts for the sparse fiber formation. The few nanofibers that were produced tended to grow in the form of short tubular structures and, as a consequence, did not project very far from the silica support surface. The graphite-supported cobalt particles exhibited a remarkable difference in behavior compared to that found for the Co/SiO_2 system and generated two different types of nanofibers. The set of larger nanofibers exhibited a jagged profile and had the appearance of a stack of cups with no well-defined axis, Figure 6. In contrast, the other fraction of nanofibers were much smaller in width and had the characteristics of uniform tubular structures. The larger nanofibers probably originate from the globular metal particles accumulated at the edge sites of graphite, which had sintered during reduction. The smaller nanofibers could be derived from small catalyst particles initially located on the basal plane regions of the graphite support or by a secondary growth process involving fragmentation of the larger active parent particles.

High-resolution TEM examination of the nanofibers generated in these supported cobalt samples revealed the existence of some major differences between the silica and two graphite-supported systems. The walls of the structures formed from Co/SiO_2 appeared to adopt an undulating profile where the graphite sheets were aligned in the same direction as the fiber axis. The smaller nanofibers produced from the Co/graphite and

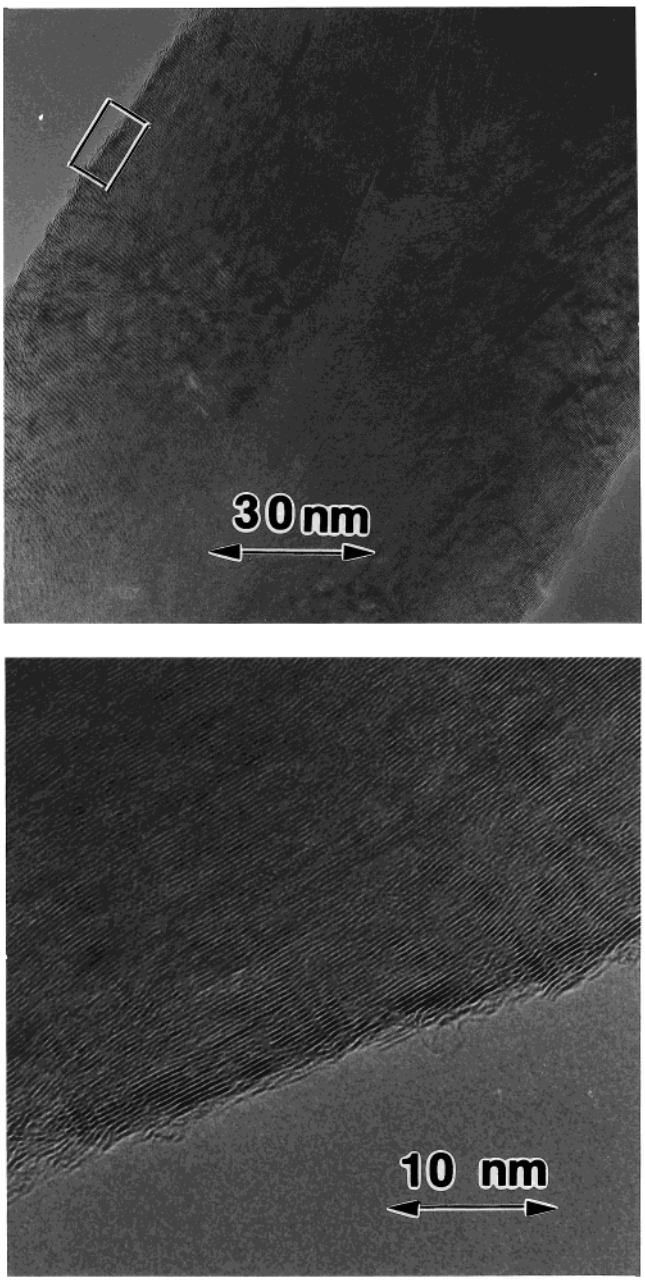

Figure 5. (a) Appearance of nanofibers generated from the decomposition of C_2H_4/H_2 (4:1) over a iron/platelet GNF catalyst system at 600 °C, and (b) an enlarged section.

Co/GNF samples tended to be more uniform in width and consisted of graphite sheets that were arranged parallel to the nanofiber growth direction. Close scrutiny of some of these structures gave the impression that some may be bundles of single-walled nanotubes.

(c) Supported Nickel Particles. These catalyst systems yielded the largest amount of solid carbon; however, the nanofibers created from this metal did not possess the same smooth profile as those generated from the supported iron samples. Widths of the fibers matched the size of the associated metal catalyst particle. These structures were of uniform density, there being no evidence for the existence of "hollow tubular" conformations.

High-resolution examination of these structures, TEM Figure 7, indicated that while the nanofibers possessed a certain degree of graphitic character, as evidenced by

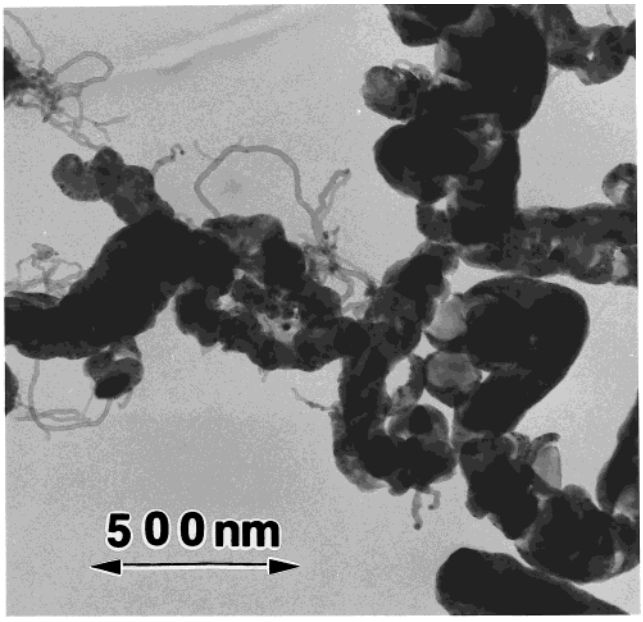

Figure 6. Appearance of carbon nanofibers generated from the interaction of Co/graphite catalyst with a C_2H_4/H_2 (4:1) mixture at 600 °C.

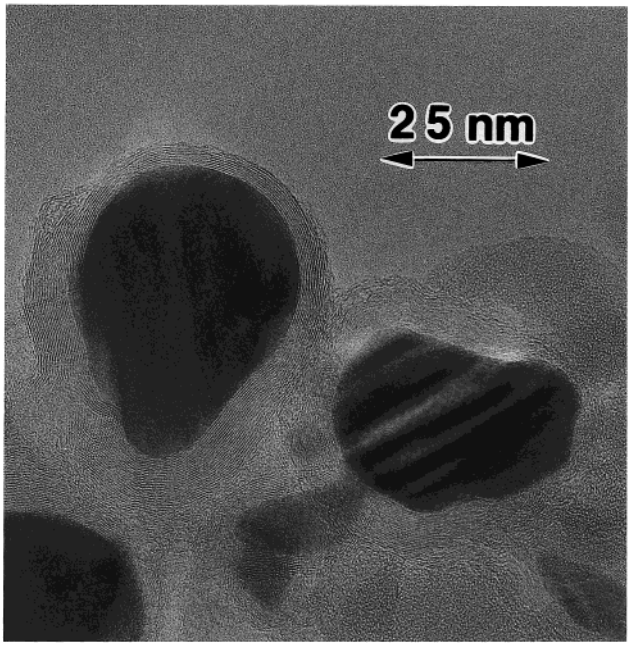

Figure 7. High-resolution electron micrograph showing the "herring bone" arrangement of nanofibers grown from the decomposition of a C_2H_4/H_2 (4:1) mixture over supported nickel particles at 600 °C.

the existence of the graphite lattice fringe images, they were somewhat less well-ordered than those generated from the other two metals. In contrast to the previous systems it was clear that the graphite platelets were not aligned parallel to the fiber axis, but instead oriented at angles to the growth direction tending to give a "herringbone" arrangement with many edge sites.

Temperature-Programmed Oxidation Studies. Because of its very nature, TEM is a subjective technique and as such, does not provide the overall information about the structure of the entire specimen. We have attempted to overcome this shortcoming by the use of temperature-programmed oxidation (TPO), a technique

Table 4. Percentage Weight Loss Due to Oxidation of Demineralized Carbons Produced with the Aid of Metal Supported Catalyst Systems

	catalyst system		
T (°C)	Co/SiO_2	Fe/SiO_2	Ni/SiO_2
400	6	2	0
500	6	2	0
600	80	4	5
700	89	5	65
800	98	23	93
900	100	42	94
1000	100	100	100

that allows one to assess the overall crystallinity of carbons. It has been established that in the absence of a metal catalyst, the onset of gasification of amorphous carbon in CO_2 occurs at 550 °C, while the corresponding point for pure graphite is 860 °C.[36] A comparison of the difference in reactivity of the various demineralized carbons is presented in Table 4. These gasification trends reveal the existence of significant differences in the characteristics of the nanofibers produced from the three catalyst systems. Carbon nanostructures generated from silica supported iron catalysts exhibited a high degree of crystallinity as shown by their resistance to oxidation; nearly 80% of the sample was still unreacted at 800 °C. On the other hand, when silica-supported cobalt or nickel were the catalysts, the conformations exhibited an entirely different gasification pattern, where over 90% of the samples were consumed when the temperature reached 800 °C, an indication that the structures were almost entirely amorphous.

Discussion

Effect of Support on Catalytic Reactivity. One of the most important aspects of this investigation is the effect that the various supports exert on the metal particles and this is manifested by a change in the characteristics of carbon nanofibers as compared to those obtained when the respective unsupported metals were reacted under the same conditions. In this context, one of the most remarkable observations was the behavior of supported iron particles. These metal particles were quite active toward nanofiber formation in a C_2H_4/H_2 environment, when the metal was dispersed on a platelet GNF carrier. This is to be contrasted with that found when unsupported iron particles were heated in the same gas mixture at 600 °C and appeared to be completely unreactive.[35] If a small amount of CO was introduced into the reactant stream, the ability of iron to decompose ethylene was drastically changed.[35,37,38]

To understand the modification in the catalytic performance of iron toward carbon nanofiber formation when the metal was in a supported condition it is necessary to refer to some of the more recent refinements in the growth mechanism of the material.[7] When metal particles are undergoing reaction in a hydrocarbon environment, reconstruction of the metal particles to acquire very definite shapes occurs. Two distinct sets of crystallographic faces are generated in the particles; one group which is capable of chemically dissociating ethylene but is unable to precipitate dis-

(36) Owens, W. T.; Rodriguez, N. M.; Baker, R. T. K. *J. Phys. Chem.* **1992**, 96, 5048.
(37) Burke, M. L.; Madix, R. J. *Surf. Sci.* **1990**, *115*, 20.
(38) Burke, M. L.; Madix, *J. Am. Chem. Soc.* **1991**, *113*, 1475.

solved carbon atoms, and another set of faces that exhibits the reverse properties. The result of these two simultaneously operating steps is that certain metal faces always remain free of solid carbon and therefore, are available for continued decomposition of the hydrocarbon. Since the geometry of the particle ultimately determines the morphology of the nanofiber, the presence of a support can drastically alter the initial shape of the catalyst and this feature will be manifested in the final structure of the solid carbon product. On the basis of the arguments presented above one may rationalize the observed modification in the carbon-depositing characteristics of iron according to the notion that in the silica-supported condition, surface atom reconstruction of particles is facilitated and crystallographic faces are generated at the metal/gas interface that favor dissociative chemisorption of ethylene.

There is clearly a significant difference in the catalytic activity of iron toward carbon nanofiber growth when supported on the different substrate materials (Figure 1). The optimum activity was achieved with all the systems after about 30 min on stream. Subsequent deactivation of the Fe/graphite and Fe/SiO_2 catalysts was observed after a reaction time of 120 min. In contrast, the performance of the metal was maintained for a longer period of time on the platelet GNF. This observed difference in activity patterns in the Fe/graphite and Fe/GNF systems is at first sight somewhat perplexing, since after a short period of time the active metal particles are located at the growing end of the nanofibers and as such, are no longer in contact with the original support media. One can argue that the differences in crystallographic features of the particles that are achieved by supporting iron on the GNF edge sites as compared to the basal plane regions encountered in SP1 graphite are "locked into the catalyst" during the nanofiber growth process, i.e., the particles retain their shapes. For the silica-supported system, one must also take into consideration that during the initial stages of the reaction the particles are in direct contact with the support and the possibility exists for insertion of silicon species into the metal. Incorporation of as little as 1 wt % of silicon into iron results in the reduction of the solubility of carbon by 50 and also has an impact on the rate of carbon diffusion through the metal.[39]

Furthermore, it is an interesting exercise to contrast the activity pattern found for the Fe/GNF− C_2H_4/H_2 (4:1) system with that obtained in a previous study in which the same catalyst combination was reacted in a $CO/C_2H_4/H_2$ (2:2:1) mixture at 600 °C.[40] Under these conditions catalytic activity toward nanofiber growth was sustained at the maximum level for a much longer period of time, showing the promotional effect of CO. It was argued that the presence of adsorbed CO could overcome the tendency of the surface of the iron particles to undergo relaxation to an arrangement that does not favor adsorption and decomposition of ethylene.

Effect of Support on the Sizes of Carbon Nanofibers. Examination of the data presented in Table 3 shows that the width of nanofibers produced from the three supported nickel systems were in the same range. Such a relationship indicates that the metal particle growth characteristics on the silica and carbonaceous materials were also very similar. Previous studies have demonstrated that under reducing conditions nickel exhibits a strong interaction with both the basal plane and edge sites of graphite[31,32] and since these are the predominantly exposed regions of SP1 graphite and platelet GNF, respectively, it is not surprising to find that the same sizes of nanofibers are generated from these two systems. A detailed investigation of the surface migration of nickel on silica was carried out by Arai and coworkers[41] using postreaction TEM examination of specimen that were treated at 600 °C over a period of 4 h. It was significant that the metal particle size distribution did not change to any appreciable extent during this treatment, suggesting the existence of a relatively strong interaction between nickel and silica.

The dramatic difference in the widths of nanofibers generated from metal particles dispersed on SP1 graphite and platelet GNF was remarkable. These respective patterns of behavior can be readily understood when one considers information obtained from controlled atmosphere electron microscopy (CAEM) studies performed on the Co/graphite−hydrogen system.[42] These experiments showed that while cobalt particles located on basal plane regions of graphite underwent rapid sintering at temperatures in excess of 500 °C those that accumulated at edges exhibited a wetting and spreading action a criterion associated with the existence of a strong metal/support interaction. Iron films did not readily nucleate to form discrete particles when the metal was dispersed on the basal plane of graphite. Conversely, however, CAEM studies have revealed that this process took place quite readily with particles in contact with the edge sites, suggesting that the latter locations favored the growth of iron crystallites.[43] On the basis of these observations, one would predict that the width of nanofibers grown from GNF-supported iron particles would be on average wider than those formed from the SP1 graphite-supported metal particles, which was indeed observed in practice.

Effect of Support on the Structural Characteristics of Carbon Nanofibers. From a comparison of the TPO profiles one can establish the oxidation characteristics of the nanofibers produced from the three silica supported metal catalysts. On the basis of these data it is apparent that the material produced from an iron catalyst displayed the highest level of graphitic character, whereas that grown from nickel exhibited the lowest degree of crystalline perfection. This sequence is the same as that found for carbon nanofibers generated from the reaction of ethylene/hydrogen with the respective unsupported metals.[18,35,44]

High-resolution TEM studies have shown that the nanofibers produced from these systems were composed of graphite platelets aligned in a direction parallel to the fiber axis giving the material a tubular form. This

(39) *Metal Handbook*; American Society of Metals: Metals Park, OH, 1973; Vol. 8.
(40) Rodriguez, N. M.; Kim, M. S.; Baker, R. T. K. *J. Phys. Chem.* **1994**, *98*, 13108.
(41) Arai, M.; Ishikawa, T.; Nishiyama, Y. *J. Phys. Chem.* **1982**, *86*, 577.
(42) Oh, S. G.; Baker, R. T. K. *J. Catal.* **1991**, *128*, 137.
(43) Baker, R. T. K.; Chludzinski, J. J.; Sherwood, R. D. *Carbon* **1985**, *23*, 245.
(44) Kim, M. S.; Rodriguez, N. M.; Baker, R. T. K. *J. Catal.* **1992**, *134*, 253.

is to be contrasted with that found for nanofibers generated from the interaction of CO/H_2 (4:1) with iron powder at 600 °C. Here the graphite platelets were stacked in a direction perpendicular to the fiber axis.[35] The ramifications of this difference in the orientation of graphite platelets is that in the former case, the surface of the nanofibers will consist primarily of basal plane regions, whereas in the latter materials, only edge sites will be exposed. As a consequence, these two types two of graphite nanofibers will exhibit major differences in their physical and chemical properties. These structural characteristics will also have an impact from the point of view of commercial applications; nanofibers that present the basal plane regions to the environment are likely to exhibit high electrical conductivity, whereas structures in which edge regions are exposed will be ideal candidates for adsorption and gas storage.

In contrast, only minor perturbations were found in the structural characteristics of nanofibers formed from the supported and unsupported cobalt and nickel systems. The nature of the support did exert some effect on the arrangement of the graphite platelets present in the nanofibers grown from cobalt particles, with the carbonaceous carriers tending to promote the formation of well-aligned tubular structures, whereas the arrangement of the graphitic component in the material grown from the cobalt/ silica system was not so well defined. Interestingly, some of the nanofibers generated from this latter catalyst system took the form of spiral conformations. This type of carbon nanofiber growth morphology has been observed in a number of previous studies,[18,45−48] and is generally associated with the presence of certain additives in the host metal catalyst particle. The presence of such "impurities" is believed to introduce a degree of asymmetry with respect to the carbon diffusion pattern through the catalyst particle that results in a nonbalanced precipitation process at the depositing faces of the metal. In the present system it is possible that this modification in nanofiber growth characteristics is attributable to the entrapment of a small fraction of silica species into the active cobalt particles.

It was difficult to identify any significant differences in any of the nanofibers created on nickel particles. While there was some evidence that the nanofibers possessed a certain degree of crystalline character where the graphite sheets were oriented in a "herringbone" arrangement, this pattern did not extend throughout the structure. The crystallinity of carbon nanostructures has been found to be dependent on a number of parameters, including the nature of the catalyst, the reactant gas, and the temperature. It has been postulated that even if the metal particle reconstructs to generate faces that match the structure of the basal plane of graphite, crystalline carbon may not be formed. The generation of graphitic structures, is achieved when the particle has reached conditions where it undergoes a wetting and spreading action on the graphite edge sites. With the aid of CAEM, iron particles were observed to wet and spread on graphite at 575 °C,[43] and this may explain the highly crystalline nature of the nanofibers produced with this catalyst. In contrast, nickel was reported to undergo spreading at temperatures in excess of 975 °C.[32] Under the present experimental conditions (600 °C), it is probable that neither nickel nor cobalt are capable of undergoing a wetting and spreading action on the graphite edge sites and as a consequence, these metal particles will tend to adopt a globular geometry, which will culminate in the growth of disordered nanofiber structures.

Since both the degree of crystalline perfection and orientation of the graphite platelets that constitute some of the nanofiber structures are controlled by the arrangement of metal atoms found at the catalyst/solid carbon interface,[7,49] it is reasonable to expect that the nature of the metal/support interaction will play a significant role in the growth process. The selection of a suitable support medium for the metal catalyst opens up new approaches that allows for the manipulation of the structural characteristics of carbon nanofibers.

Summary

The results of this investigation have demonstrated that major modifications in the growth characteristics of carbon nanofibers can be achieved when iron, cobalt, and nickel are used in a supported rather than powdered form to catalyze the decomposition of ethylene at 600 °C. Moreover, there were significant differences in the performance of these metals depending upon the nature of the metal−support interaction. In this respect, one of the most intriguing findings was that while powdered iron samples did not generate carbon nanofibers from ethylene/hydrogen mixtures, when the metal was dispersed on either silica, graphite, or graphite nanofiber supports, the growth of these structures proceeded in a very facile manner.

High-resolution transmission electron microscopy studies of the solid carbon deposit formed in these reactions revealed that nanofibers were the exclusive product with no other forms of carbon being present. Examination of the detailed structural characteristics of the nanofibers grown from the various supported metals indicated that those produced from iron catalysts exhibited the highest degree of crystalline perfection. In all cases, the nanofibers derived from iron adopted a structure in which the graphite platelets were aligned in a direction parallel to the fiber axis. Close inspection showed that these nanofibers were not rounded, but instead acquired a faceted outline, where the wall thicknesses varied from a single to multiple graphite sheets. It was fascinating to find that this nanofiber geometry was maintained even when such "secondary" structures were generated from iron particles supported on "parent" graphite nanofibers where the graphite sheets were aligned in a direction perpendicular to the fiber axis.

Acknowledgment. This work was supported by the U.S. Department of Energy, Grant 96ER41688. The authors also thank Mike Frongillo, CMSE EM Center at MIT for some of the HRTEM work.

CM990582N

(45) Kawaguchi, M.; Nozaki, K.; Motojima, S.; Iwanaga, H. *J. Cryst. Growth* **1992**, *118*, 309.
(46) Motojima, S.; Hasegawa, I.; Kagiya, S.; Momiyama, M.; Kawaguchi, M.; Iwanaga, H. *Appl. Phys. Lett.* **1993**, 62, 2322.
(47) Owens, W. T.; Rodriguez, N. M.; Baker, R. T. K. *Catal. Today* **1994**, *21*, 3.
(48) Park, C.; Baker, R. T. K. *J. Catal.* **1998**, *179*, 361.
(49) Rodriguez, N. M.; Kim, M. S.; Baker, R. T. K. *J. Catal.* **1993**, *143*, 449.